



ELSEVIER

Journal of Non-Crystalline Solids 273 (2000) 209–214

JOURNAL OF
NON-CRYSTALLINE SOLIDS

www.elsevier.com/locate/jnoncrysol

Laser spectroscopy and electron paramagnetic resonance of Cr^{3+} doped silicate glasses

V.C. Costa ^{a,*}, F.S. Lameiras ^a, M.V.B. Pinheiro ^a, D.F. Sousa ^b, L.A.O. Nunes ^b,
Y.R. Shen ^c, K.L. Bray ^c

^a CDTN/CNEN-Centro de Desenvolvimento da Tecnologia Nuclear, CP 941, Pampulha, 30123-970, Belo Horizonte, MG, Brazil

^b Instituto de Física de São Carlos, USP, CP 369, 13570-970, São Carlos SP, Brazil

^c Department of Chemistry and Institute for Shock Physics, Fulmer Hall, Washington State University, Pullman, WA 99164, USA

Abstract

Gels and glasses in the $\text{SiO}_2\text{-Al}_2\text{O}_3\text{-ZnO-Cr}_2\text{O}_3$ and $\text{SiO}_2\text{-Al}_2\text{O}_3\text{-MgO-Cr}_2\text{O}_3$ systems were synthesized by the sol-gel method. A description of the change of the Cr^{3+} environment during the xerogel-glass-glass ceramic transformation is presented using optical properties of Cr^{3+} ions. Absorption and emission spectra, electron paramagnetic resonance measurements, and site-selective laser spectroscopy were performed to characterize the Cr^{3+} fluorescent centers. Absorption and fluorescence are interpreted by structural considerations showing the variation of Cr^{3+} environment during heat treatment. By heating glasses, the glass-ceramics containing chromium-doped ZnAl_2O_4 (gahnite) are formed. The results indicate the presence of chromium ions in a gahnite crystalline phase and emission from the ${}^2\text{E}$ level is observed. Also a Cr^{3+} fluorescence centered at 770 nm results from ${}^4\text{T}_2$ level of Cr^{3+} sites at low ligand field in glassy phase. © 2000 Elsevier Science B.V. All rights reserved.

1. Introduction

Gel-glass crystallization studies have been performed using transition metals ions as nucleating agents and spectroscopic probes [1,2]. This area of research is about control of physical and optical properties through controlled crystallization of phases in glass matrices [3].

Cr^{3+} ion is a nucleating agent for the formation of crystalline phases and has fluorescence properties that make it an effective local probe [3,4]. In glass phases, Cr^{3+} ions occupy a variety of sites with different crystal field strengths due to site

variability and compositional disorder [2]. The first excited state is ${}^2\text{E}$ in high field sites and ${}^4\text{T}_2$ in low field sites [5]. The relative energies of the excited ${}^4\text{T}_2$ and ${}^2\text{E}$ states depend on the crystal field strength.

In silicate glasses both high and low field Cr^{3+} sites have been observed [2,6,7]. Simultaneous emission from the ${}^2\text{E}$ and ${}^4\text{T}_2$ levels occurs and the emissions have been shown to lase [8]. Cr^{3+} has also been demonstrated to be an effective sensitizer of Nd^{3+} emission in both glasses and glass-ceramics [9,10].

Low field Cr^{3+} sites are primarily observed in silicate glasses [6,11] and from which ${}^4\text{T}_2 \rightarrow {}^4\text{A}_2$ emission occurs as a band in the near infrared at 850 nm. In silicate glass-ceramics, Cr^{3+} preferentially nucleates in the crystalline phase and is in sites which produce the high field condition

* Corresponding author. Tel.: +55-31 499 3235; fax: +55-31 499 3390.

E-mail address: vilma@urano.cdtm.br (V.C. Costa).

[12,13]. The spectrum of high field Cr^{3+} in both glasses and glass-ceramics consists of structured ${}^2\text{E} \rightarrow {}^4\text{A}_2$ emissions which have high quantum efficiencies [2,7].

In this work, xerogel samples of the SiO_2 – Al_2O_3 – ZnO (or MgO)– Cr_2O_3 systems were prepared from the sol–gel process. In these systems, Cr^{3+} is a nucleating agent and glass-ceramics are nucleated by it. We report the results of optical absorption, emission and EPR measurements and analyse the local structural changes that occur in the vicinity of Cr^{3+} during the glass to glass-ceramic transformation.

2. Experimental

2.1. Sample preparation

The silicate gels were prepared by combining tetramethoxysilane (TMOS) with an aqueous solution in which nitrate salts were previously dissolved [14]. Aluminum nitrate, $\text{Al}(\text{NO}_3)_3 \cdot 9\text{H}_2\text{O}$, zinc nitrate, $\text{Zn}(\text{NO}_3)_2 \cdot 6\text{H}_2\text{O}$, or magnesium nitrate, $\text{Mg}(\text{NO}_3)_2 \cdot 6\text{H}_2\text{O}$, were used as the starting reagents. The nitrates of Al and Zn were dissolved at 50°C. Chromium nitrate was also added. The TMOS was added to the aqueous salt solution under constant stirring. Stirring was continued at 50°C for 1 h. Afterwards, samples were cast in plastic vials and allowed to react at room temperature. After gelation, the samples were aged at 60°C for 2 days and then dried at 90°C for 2 days. Heat treatment at temperatures between 100°C and 975°C was performed in a nitrogen controlled atmosphere.

Salt concentrations were adjusted to give the compositions $x\text{SiO}_2$ – $y\text{Al}_2\text{O}_3$ – $z\text{ZnO}$ or MgO – $c\text{Cr}_2\text{O}_3$, where $70 < x < 89$, $6 < y < 19.5$, $4.9 < z < 10$, $c = 0.1$, 0.2 and 0.5. Samples heated to 800°C or 975°C were transparent. Precipitation was occasionally observed, especially in compositions which had less than 85% mol SiO_2 .

2.2. Physical measurements

X-ray diffraction was carried out with a diffractometer (Rigaku model Geighflex) using a

CuK_α radiation as a source. Optical absorption was measured with a spectrophotometer (Toshiba U-3510) in the wavelength range of 200–3200 nm. EPR spectra were measured at 30 K using a X-band (9.5 GHz) spectrometer equipped with a cylindrical cavity (Bruker) and a He-flow cryostat (Oxford systems).

Fluorescence of Cr^{3+} was excited with an argon-pumped dye laser or with the 514.5 nm line of an argon ion laser. The dye laser provided emission from 457 to 670 nm, depending on the dye (coumarin, rhodamine and DCM). The excitation source for the time resolved spectroscopy measurements, at 5 K, was a Q-switched Nd:YAG laser. For the luminescence decay measurements, the near infrared Cr^{3+} emission was passed through a 0.3 m monochromator detected by a Ge detector and recorded by a digital storage oscilloscope. In the red range, the signal was recorded with a triple monochromator and an optical multichannel analyzer. A dye laser pumped by a pulsed nitrogen laser was used as the excitation source for fluorescence measurements in the red.

3. Results

We observed that chromium oxidizes from Cr^{3+} at low temperature to Cr^{6+} in all samples upon heating in air to 800°C. This change was detected by a change in color from green to yellow [15] and the appearance of the absorption spectra of the heated samples. To minimize Cr^{6+} contamination, the samples were heated in a nitrogen atmosphere established by flushing the furnace 1 h before.

In the X-ray diffraction experiments crystallization in the samples upon heating for 4 h at 700°C was not detected. At 850°C crystallization occurs and the gahnite phase (ZnO – Al_2O_3) was observed in samples containing ZnO. No evidence of quartz formation was observed in samples containing ZnO upon heating for 2 h at 950°C. No crystalline phases were detected in samples containing MgO after heat treatments up to 850°C (5 h). Samples containing MgO and 70 mol% SiO_2 formed quartz after 2 h at 950°C. Samples containing MgO had less tendency to crystallize and are not discussed further in this paper.

Most of the measurements presented in this paper are based on the $89\text{SiO}_2\text{--}5.9\text{Al}_2\text{O}_3\text{--}4.9\text{ZnO}\text{--}0.2\text{Cr}_2\text{O}_3$ composition. The X-ray pattern for this sample showed that the gahnite phase was formed during heat treatment with a simultaneous change in color from green to pink during crystallization.

3.1. Absorption

The absorption spectrum of Cr^{3+} in gels dried at 100°C is shown in Fig. 1(a). The absorption spectrum in the xerogels before heat treatment consists mainly of two peaks at ~ 580 and ~ 415 nm. These bands are due to the absorption transitions from the ${}^4\text{A}_2$ ground state of Cr^{3+} ions to the ${}^4\text{T}_2$ and ${}^4\text{T}_1$ excited states, respectively, and are attributed to the presence of Cr^{3+} in six-coordinate bonding sites [11]. A shoulder was also recorded at 680 nm.

Figs. 1(b) and (c) show absorption spectra for two heat treated samples containing ZnO. The

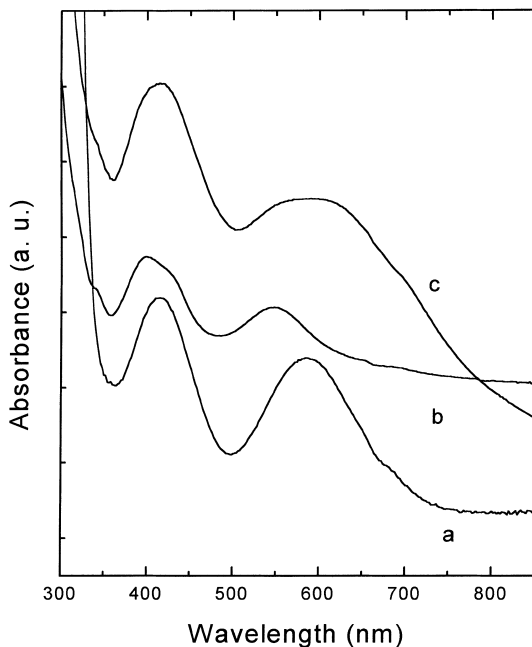


Fig. 1. Absorption spectra at room temperature: (a) $89\text{SiO}_2\text{--}5.9\text{Al}_2\text{O}_3\text{--}4.9\text{ZnO}\text{--}0.2\text{Cr}_2\text{O}_3$ (xerogel heated to 100°C); (b) $89\text{SiO}_2\text{--}5.9\text{Al}_2\text{O}_3\text{--}4.9\text{ZnO}\text{--}0.2\text{Cr}_2\text{O}_3$ heated to 850°C for 5 h; (c) $83.3\text{SiO}_2\text{--}9.25\text{Al}_2\text{O}_3\text{--}7.25\text{ZnO}\text{--}0.2\text{Cr}_2\text{O}_3$ heated to 750°C for 3 h.

sample of Fig. 1(b) is a glass ceramic with the composition $89\text{SiO}_2\text{--}5.9\text{Al}_2\text{O}_3\text{--}4.9\text{ZnO}\text{--}0.2\text{Cr}_2\text{O}_3$. In this sample, the maximum of the ${}^4\text{A}_2 \rightarrow {}^4\text{T}_2$ transition is shifted to shorter wavelengths relative to an unheated sample. The ${}^4\text{A}_2 \rightarrow {}^4\text{T}_1$ transition also has a noticeable splitting ($\lambda = 420$ and $\lambda = 372$ nm). The sample shown in Fig. 1(c) was heated to a temperature below which crystallization occurs. This sample is amorphous and, except for peak broadening, its spectrum is similar to that shown for the gel (Fig. 1(a)). A charge transfer absorption band near 343 nm can also be seen and is due to Cr^{6+} ions in tetrahedral symmetry [16].

3.2. Fluorescence

Fig. 2 shows the 5 K emission spectrum of Cr^{3+} in $89\text{SiO}_2\text{--}5.9\text{Al}_2\text{O}_3\text{--}4.9\text{ZnO}\text{--}0.2\text{Cr}_2\text{O}_3$ heated to 850°C for 3 h, upon excitation with an argon laser at $\lambda_{\text{exc}} = 514$ nm. The observed emission spectrum is similar to that reported for Cr^{3+} in gahnite (ZnAl_2O_4) [17] with features directly attributable to previously determined Cr^{3+} multisites with both weak and strong crystal fields (see Fig. 2 for labelling of sites) [18].

Fig. 3 shows the 5 K emission at several excitation wavelengths: 457, 514, 615 and 670 nm. Upon excitation at 670 nm ($14,925\text{ cm}^{-1}$), a fluorescence band with larger amplitude peaking at ~ 770 nm ($13,000\text{ cm}^{-1}$) was observed. The low energy excitation wavelength selectively excited Cr^{3+} ions in the weak field amorphous phase of the glass-ceramic. The emission is attributed to the ${}^4\text{T}_2 \rightarrow {}^4\text{A}_2$ transition.

Increasing the excitation energy to 615 nm produced an emission band near 700 nm ($14,286\text{ cm}^{-1}$) as well as smaller emission amplitude at longer wavelengths. At 615 nm ($16,260\text{ cm}^{-1}$), excitation occurs into the high energy tail of the amorphous phase ${}^4\text{A}_2 \rightarrow {}^4\text{T}_2$ absorption band (see inset of Fig. 3) and the broad emission is attributed to ${}^4\text{T}_2 \rightarrow {}^4\text{A}_2$ emission from low field Cr^{3+} sites in the amorphous phase. The larger amplitude emission at shorter wavelengths is attributed to ${}^2\text{E} \rightarrow {}^4\text{A}_2$ emission from high field Cr^{3+} sites in the amorphous phase [2] and a small contribution from Cr^{3+} ions in the high field gahnite microcrystalline phase.

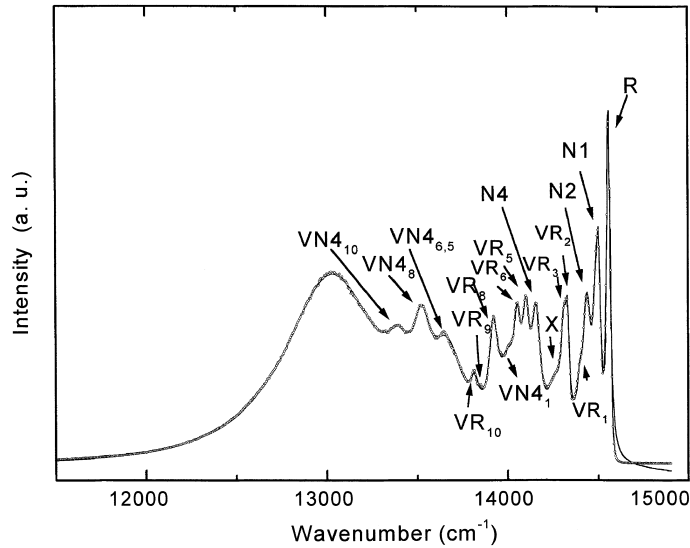


Fig. 2. Emission spectrum of Cr^{3+} in gahnite glass-ceramic at $\lambda_{\text{exc}} = 514 \text{ nm}$, $T = 5 \text{ K}$. The labels R and N designate distinct Cr^{3+} bonding sites [18] and V designates a vibronic satellite peak.

At 457 and 514 nm, excitation occurs primarily into the ${}^4\text{A}_2 \rightarrow {}^4\text{T}_2$ band of Cr^{3+} in the high field gahnite phase. The width of the emission is consistent with Cr^{3+} emission in a crystalline environment [18] and we attribute it to the ${}^2\text{E} \rightarrow {}^4\text{A}_2$ transition. The spectral features observed upon

457 nm or 514 nm excitation are similar to that previously reported for $\text{Cr}^{3+}:\text{ZnAl}_2\text{O}_4$ [17,18]. The band underlying these features and the longer wavelength band are attributed to high and low field Cr^{3+} sites, respectively, in the amorphous phase [2].

The lifetimes of the R , N_1 , N_2 , and N_4 lines of the sample shown in Fig. 3 (see Fig. 2 for designation of spectral lines) were measured under pulsed laser excitation at 532 nm. The lifetimes of the four lines were slight non-exponential with lifetimes of 12, 10, 8 and 1 ms for the R , N_1 , N_2 , and N_4 lines, respectively.

In the EPR spectra of the glasses, four components were observed. In Fig. 4, we show the EPR spectrum of Cr^{3+} in the composition $89\text{SiO}_2 - 5.9\text{Al}_2\text{O}_3 - 4.9\text{ZnO} - 0.2\text{Cr}_2\text{O}_3$ as a glass-ceramic (heat treated at 950°C for 2 h, Fig. 4(a)) and a glass (heat treated at 750°C for 3 h, Fig. 4(b)). The spectrum for the glass ceramic sample has an absorption at $H = 0.35 \text{ T}$ ($g \approx 2.0$), which we assign to coupled Cr^{3+} pairs in the glassy phase [19,20] and an asymmetric absorption around $H = 0.16 \text{ T}$ ($g \approx 5.0$), which we attribute to Cr^{3+} in the gahnite phase [12]. The EPR spectrum for the glass removed from heating prior to crystallization shows a signal with smaller width near $H = 0.35 \text{ T}$,

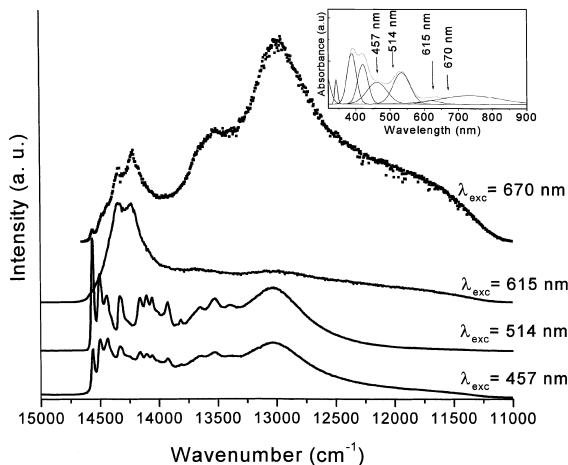


Fig. 3. 5 K emission spectra of the Cr^{3+} ion in $89\text{SiO}_2 - 5.9\text{Al}_2\text{O}_3 - 4.9\text{ZnO} - 0.2\text{Cr}_2\text{O}_3$ heated to 850°C for 3 h. Emission spectra at four excitation wavelengths are shown. The inset shows the location of the excitation wavelengths relative to the absorption spectrum.

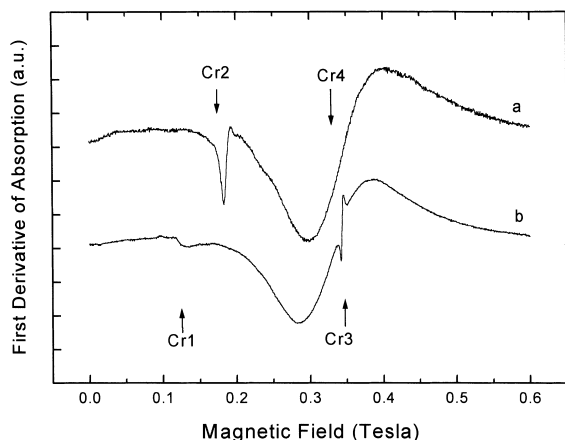


Fig. 4. EPR spectra at 30 K of $89\text{SiO}_2\text{-}5.9\text{Al}_2\text{O}_3\text{-}4.9\text{ZnO-}0.2\text{Cr}_2\text{O}_3$ as (a) a glass-ceramic containing a gahnite phase and (b) a glass heated below the onset of crystallization. Features associated with Cr^{3+} in the glassy phase (Cr1), Cr^{3+} in the gahnite phase (Cr2), isolated Cr^{5+} ions (Cr3), and Cr^{3+} exchanged-coupled pairs (Cr4) are indicated.

which we assign to isolated Cr^{5+} ions [21,22], a smaller amplitude absorption near $H = 0.12$ T we attributed to isolated Cr^{3+} ions in distorted sites of the glassy phase [20], and the absorption at $g \approx 2.0$ with a larger width, also seen in the glass-ceramic sample, is attributed to exchange coupled Cr^{3+} pairs in the glassy phase [19,20].

4. Discussion

4.1. Absorption

From the absorption spectra of Fig. 1, both the ${}^4\text{T}_2$ and ${}^4\text{T}_1$ levels of Cr^{3+} in the gahnite crystalline phase of the glass ceramic are shifted to higher energy in comparison to the glass phase. This shift indicates that Cr^{3+} in the crystalline phase is in a site with a crystal field with larger $10 D_q$ and shorter average bond lengths to the nearest neighbor oxygen ligands [23].

The energy corresponding to the band peaks may be used to determine the strength of the octahedral crystal field, D_q , experienced by the Cr^{3+} ions and the electron–electron repulsion parameters, B and C . These are averages over the distribution of sites occupied by the Cr^{3+} ions in glasses.

From the ${}^4\text{A}_2 \rightarrow {}^4\text{T}_1$ and ${}^4\text{A}_2 \rightarrow {}^4\text{T}_2$ absorption maxima, the D_q/B was found to be 2.71 using standard Tanabe–Sugano theory [24]. The $D_q/B = 2.71$ is consistent with high field Cr^{3+} in the gahnite crystalline phase and the presence of ${}^2\text{E} \rightarrow {}^4\text{A}_2$ emission, as observed in Fig. 2.

4.2. Fluorescence

Excitation at 514 nm results in lines that we attribute to the zero phonon (R, N_i) and vibronic sideband ($VR_i, VN_{i,j}$) lines of the ${}^2\text{E} \rightarrow {}^2\text{A}_2$ transition. The R and N_i lines have been discussed in previous work [6,7]. The lines are emitted from the ${}^2\text{E}$ level of high field Cr^{3+} in the crystalline gahnite phase. The spectral features are consistent with Cr^{3+} occupying sites of approximate O_h symmetry [18]. The R line is from the principle Cr^{3+} bonding sites. The longer R line lifetime (12 ms) indicates that the principle Cr^{3+} bonding site has a symmetry which is close to regular octahedral [25]. The N_1 and N_2 lines are from smaller concentrations of Cr^{3+} in sites which are perturbed to a greater extent from octahedral symmetry. The N_4 line is from paired Cr^{3+} ions [25]. The broad emission centered at 770 nm and extending up to 800 nm we assign to ${}^4\text{T}_2 \rightarrow {}^4\text{A}_2$ transition of Cr^{3+} sites at low ligand field in glassy phase [6]. The EPR measurements confirm the presence of Cr^{3+} pairs and multiple Cr^{3+} environment in the glassy and crystalline phases.

5. Conclusions

We have carried out spectroscopic, X-ray and EPR measurements on Cr^{3+} in systems with composition $\text{SiO}_2\text{-Al}_2\text{O}_3\text{-ZnO-Cr}_2\text{O}_3$ and $\text{SiO}_2\text{-Al}_2\text{O}_3\text{-MgO-Cr}_2\text{O}_3$ prepared from the sol–gel process. Heat treatment of xerogels of the former composition above 850°C led to the formation of gahnite (ZnAl_2O_4) phase. We have shown from luminescence and decay measurements that Cr^{3+} readily incorporates in high field bonding sites of the crystalline phase. An increase in Cr^{3+} quantum efficiency occurs upon incorporation into the crystalline phase. The latter composition was not observed to crystallize.

Acknowledgements

The authors acknowledge financial support from FAPEMIG. V.C.C. acknowledges Professor Mauro L. Baesso and K. Krambrock. K.L.B. and Y.R.S. acknowledge primary financial support from the US National Science Foundation and partial financial support from the US Department of Energy.

References

- [1] L.J. Andrews, G.H. Beall, A. Lempicki, *J. Lumin.* 36 (1986) 65.
- [2] G. Boulon, *Mater. Chem. Phys.* 16 (1987) 301.
- [3] W. Nie, G. Boulon, C. Mai, C. Esnouf, Xu Ruanjuan, J. Zarzycki, *Chem. Mater.* 4 (1992) 216.
- [4] G.F. Imbusch, *Phys. Scripta* T19 (1987) 354.
- [5] B. Henderson, G.F. Imbusch, *Optical Spectroscopy of Inorganic Solids*, Oxford Science, New York, 1989.
- [6] L.J. Andrews, A. Lempicki, B.C. McCollum, *J. Chem. Phys.* 74 (1981) 5526.
- [7] F. Rasheed, K.P. O'Donnell, B. Henderson, D.H. Hollis, *J. Phys.: Condens. Matter* 3 (1991) 1915.
- [8] R. Reisfeld, *Mater. Sci. Eng.* 71 (1985) 375.
- [9] M.D. Shin, A.A. Tesar, *J. Lumin.* 51 (1992) 189.
- [10] G. Armagan, B. DiBartolo, *IEEE J. Quant. Electron.* 24 (1988) 974.
- [11] S.A. Brawer, W.B. White, *J. Chem. Phys.* 67 (1977) 2043.
- [12] A. Kisilev, R. Reisfeld, E. Greenberg, A. Buch, M. Ish-Shalom, *Chem. Phys. Lett.* 129 (5) (1986) 450.
- [13] F. Durville, B. Champagnon, E. Duval, G. Boulon, *J. Phys. Chem. Solids* 46 (1985) 70.
- [14] V.C. Costa, M.J. Lochhead, K.L. Bray, *Chem. Mater.* 8 (3) (1996) 783.
- [15] F.H. Norton, *Elements of Ceramics*, Addison-Wesley, Reading, MA, 1974.
- [16] J.S. Stroud, *J. Am. Ceram. Soc.* 54 (1971) 401.
- [17] W. Mikenda, A. Preisinger, *J. Lumin.* 26 (1982) 67.
- [18] W. Nie, F.M. Michel-Calenfina, C. Linares, G. Boulon, C. Daul, *J. Lumin.* 46 (1990) 177.
- [19] R.J. Laundry, J.T. Fournier, C.G. Young, *J. Chem. Phys.* 46 (1967) 1285.
- [20] E.A. Harris, *Phys. Chem. Glasses* 28 (1987) 196.
- [21] N. Iwanoto, Y. Makino, *J. Non-Cryst. Solids* 41 (1980) 257.
- [22] D.L. Griscom, *J. Non-Cryst. Solids* 40 (1980) 211.
- [23] R.E. Tischer, *J. Chem. Phys.* 48 (1968) 4291.
- [24] S. Sugano, Y. Tanabe, H. Kamimura, *Multiplets of Transition-Metal Ions in Crystals*, Academic Press, New York, 1970.
- [25] W. Mikenda, *J. Lumin.* 26 (1981) 85.